Proceedings of the IASTED International Conference
Signal and Image Processing (SIP'99)
October 18-21, 1999, Nassau, Bahamas

On Asymptotic Properties of Frequency Warped Wavelets

GIANPAOLO EVANGELISTA, École Polytechnique Fédérale de Lausanne, Switzerland, gianpaolo.evangelista@epfl.ch
SERGIO CAVALIERE, Department of Physical Sciences, Univ. of Naples "Federico II", Italy, cavaliere@na.infn.it

Abstract

In this paper we study asymptotic properties of frequency warped wavelets defined by means of iterated warping. These wavelets are based on the iteration of a structure consisting of a two-channel perfect reconstruction, orthogonal filter bank and a Laguerre transform block. In particular, we show that 1) the sequence of Laguerre parameters determined by the exponential cutoff choice $\omega_n = a^n\pi$ converges for $0<a<1$; 2) the normalized map converges to a differentiable function uniformly on compact sets and 3) the asymptotic warping map satisfies Schröder's equation. We provide an extension of Königs's model to parametric maps on the unit circle. In our construction, we exploit the resulting conjugacy properties to define continuous-time warped wavelets and to show that these wavelets correspond to scale-a wavelets. We also show that the characteristic warping function is related to a self-similar map.

Keywords: Wavelets, Frequency Warping, Laguerre Transform, Schröder's Equation, Königs's Model.

1. Introduction

In recent papers [6, 7] the authors defined a family of dyadic wavelets having arbitrary bandwidth. These wavelets can be obtained from ordinary wavelets by means of iterated frequency warping. The allocation of the analysis bands is controlled by means of a discrete set of Laguerre parameters. Flexibility in the bandwidth design makes these wavelets particularly suitable for applications in signal processing [10]. In fact, it is well know that the octave-band frequency resolution of dyadic wavelets is very poor. Attempt to increase the resolution resulted in wavelets based on rational sampling rate filter banks whose design is difficult when constrained by asymptotic properties of the wavelets such as regularity [4].

Frequency warped wavelets can be adapted to signals or to perceptual characteristics. For digital audio applications we showed that it is possible to construct perfect reconstruction orthogonal filter banks based on perceptual bands [8], e.g., as in Bark scale. Other applications include adaptation of the Pitch-Synchronous wavelet transform to unevenly spaced harmonics typical of stationary waves in dispersive media. This allows us to resolve transient and noise from pseudo-harmonic components in inherently inharmonic sounds [5, 9].

Continuous-time frequency warped wavelets were first introduced by Baraniuk and Jones who exploited unitary equivalence to show that the warped wavelets are orthogonal and complete [3]. Their set is based on a single warping map acting on the wavelets. In their paper, little detail is given to the realization in digital structures. Our construction is based on iteration of a frequency warped filter bank, shown in Fig. 1. In the analysis section the signal is discrete Laguerre transformed (LT) and the Laguerre coefficients are passed through a 2-band orthogonal filter bank (QMF). The synthesis structure consists of the inverse filter bank cascaded by inverse Laguerre transform (ILT). We showed in [7] that warping the signal is equivalent to warping both the transfer functions and the upsampling / downsampling operators.

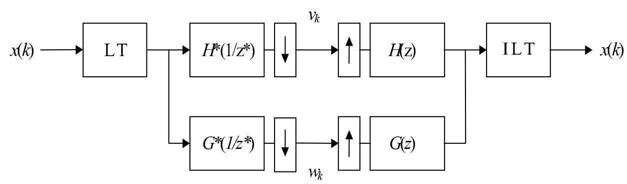

Fig. 1 *. Frequency warped filter bank structure*

It is worthwhile noting that the Laguerre transform can be factored in rational transfer functions as a cascade of first order all-pass filters [1, 2]. Therefore our construction generates wavelets that can be directly implemented in digital systems. We showed in [7] that our choice is the unique one-to-one warping map having this property.

The Laguerre transform is characterized by a single-parameter family of warping maps. By choosing the Laguerre parameter one can arbitrarily displace the cutoff frequency of the warped filter bank, the identical map being given by setting the Laguerre parameter to 0, with a cutoff of $\pi/2$ (half-band filters) of the QMF. For higher frequency resolutions, i.e., for obtaining a smaller bandwidth of the high-pass filter, one must choose negative values of the parameter. The frequency warped filter bank is iterated by cascading identical sections -- possibly with distinct parameters -- to the low-pass branch of the previous section. In this way we obtain a structure to compute the Frequency Warped Wavelet Transform. One can show [6] that the DFT of the corresponding warped scaling sequence is

$$\Phi_{N,0}(\omega) = \prod_{k=1}^{N} \left\{ \Lambda_{k,0}(2\Omega_{k-1}(\omega)) H(\Omega_k(\omega)) \right\}, \qquad (1)$$

where

$$\Omega_n(\omega) = \tfrac{1}{2}\vartheta_n \circ \vartheta_{n-1} \ldots \circ \vartheta_1(\omega) \qquad (2)$$

is the iterated warping map, composition of the elementary maps

$$\vartheta_n(\omega) = 2\omega + 4\tan^{-1}\frac{b_n \sin\omega}{1 - b_n\cos\omega}\ , \ -1 < b_n < 1\ , \qquad (3)$$

b_n are the Laguerre parameters and

$$\Lambda_{k,0}(\omega) = \frac{\sqrt{1-b_k^2}}{1-b_k e^{-j\omega}}.$$

The function $-\frac{1}{2}\vartheta_n(\omega)$ is the phase of a stable first-order all-pass filter with pole in $z = b_n$.

Unlike discrete dyadic wavelets, warped wavelets at fixed scale level are not obtained by shifting the same sequence. Rather, level N scaling sequences (and wavelets) are related to each other by all-pass filtering, according to the following relationship:

$$\Phi_{N,m}(\omega) = e^{-j2m\Omega_N(\omega)}\Phi_{N,0}(\omega) \quad (4)$$

Given a choice for the cutoff frequencies $\omega_1 > \omega_2 > .... > \omega_N$, the corresponding Laguerre parameters b_n are obtained by means of the following recurrence:

$$b_1 = \tan\left(\tfrac{\pi-2\omega_1}{4}\right),$$
$$b_n = \tan\left(\tfrac{\pi}{4} - \Omega_{n-1}(\omega_n)\right), \qquad n=2,3,...$$

The complexity of the map makes its analysis a difficult problem. A case of interest is given by selecting exponential cutoff frequencies $\omega_n = \pi a^n$, where $0<a<1$. This choice is derived from the structure of dyadic wavelets and admits these as a particular case for $a=1/2$. We will show that the asymptotic properties of the warping map for large n are remarkable for this case and that warped wavelets correspond to scale-a continuous-time wavelets.

2. Schröder's Equation and Königs's Model for Parametric Maps on the Unit Circle

In this section we present results concerning the convergence of the normalized map. The complexity of the warping map requires specific tools for its analysis. Our theory is based on Königs's model [11]. This model has been extensively studied for the composition operator acting on identical maps defined in the unit disk. In order to apply this construction to iterated warping maps, we extended the theory to allow for composition of parametric maps on the unit circle. We will present the main theorems omitting their proofs.

Our principal result is summarized in the following

Theorem 1. Let $f(\omega;\eta)$ be a 1-parameter family of maps of the real line into itself, fixing the point $\omega = 0$ for any value of the parameter η. Let $f_n(\omega) \equiv f(\omega,\eta_n)$, where $\eta_n, n \in \aleph$, is a sequence of values of the parameter η such that:

- $\forall n \in \aleph$, f_n has bounded second derivatives and $|f_n'(0)| > 0$
- $|f_n(\omega)| \le \alpha_n|\omega| < |\omega|$, for all but finitely many integers n

then the sequence $\frac{F_n}{F_n'(0)}$, with $F_n \equiv f_1 \circ f_2 \circ ... \circ f_n$ and $F_n'(0) = \prod_{k=1}^{n} f_k'(0)$, converges uniformly on any compact subsets of $\Re$. Furthermore, if $f_\infty(\omega) = \lim_n f_n(\omega)$ exists finite and differentiable at $\omega = 0$ then Schröder's equation

$$F \circ f_\infty = f_\infty'(0)F$$

is satisfied by $\lim_n \frac{F_n}{F_n'(0)}$.

The previous theorem can be applied to the inverse iterated warping map

$$\Omega_n^{-1}(\omega) = \vartheta_1^{-1} \circ \vartheta_2^{-1} \circ ... \circ \vartheta_n^{-1}(2\omega),$$

where ϑ_n^{-1} belongs to the 1-parameter family

$$\vartheta^{-1}(\omega;b) = \frac{\omega}{2} - 2\tan^{-1}\frac{b\sin\frac{\omega}{2}}{1+b\cos\frac{\omega}{2}},$$

which is indefinitely differentiable with respect to ω with bounded second derivative. For our purposes it is convenient to replace the parameter b by the parameter $\nu = \frac{1-b}{1+b}$. It is easy to show that for $\nu < 1$ we have $|\vartheta^{-1}(\omega;b)| < |\omega|$ while for $\nu > 1$, $|\vartheta^{-1}(\omega;b)| < \frac{\nu}{2}|\omega|$. By a convexity argument, it is possible to show that $a < \frac{1}{2} \Leftrightarrow \nu_n < 1, \forall n \in \aleph$ and $a > \frac{1}{2} \Leftrightarrow \nu_n > 1, \forall n \in \aleph$. The case $a = \frac{1}{2}$ is trivial since it leads to the linear maps $\vartheta^{-1}(\omega;0) = \frac{\omega}{2}$ and warped wavelets revert to dyadic wavelets. Based on the previous remarks and on a fixed- point argument we were able to prove the following

Proposition 2. For any value of $a \in]0,1[$ there exists a unique sequence of parameters ν_n such that the cutoff condition $\Omega_n^{-1}(\frac{\pi}{2}) = a^n\pi$ is satisfied with $\nu_n > 0, \forall n \in \aleph$ and $\nu_n > 2$ for at most finitely many $n \in \aleph$.

In numerical computations we observed that $\nu_n < 2$ for $n > 1$. However, the results stated in Proposition 1 are enough to guarantee the applicability of Theorem 1 to our maps. Since $\frac{d}{d\omega}\Omega_n^{-1}(\frac{\omega}{2}) = \prod_{k=1}^{n}\frac{\nu_k}{2} = \lambda_n$ then the sequence $\frac{1}{\lambda_n}\Omega_n^{-1}(\frac{\omega}{2})$ converges to a map $\widetilde{\Omega}^{-1}(\omega)$ uniformly on compact subsets of $\Re$. By virtue of uniform convergence, the map $\widetilde{\Omega}^{-1}(\omega)$ is increasing and differentiable. In particular, the cutoff condition implies that for $\omega = \pi$ we have $\widetilde{\Omega}^{-1}(\pi) = \lim_n \frac{a^n\pi}{\lambda_n} = \pi\prod_{k=1}^{\infty}\frac{2a}{\nu_k}$. Therefore the product $\prod_{k=1}^{n}\frac{2a}{v_k}$ converges to $\frac{1}{\pi}\widetilde{\Omega}^{-1}(\pi)$, which implies that

$$\lim_{k} v_k = 2a \ . \quad (5)$$

This is a remarkable result since the dependency of the parameter v_k on a is highly complex. In order to appreciate this problem it suffices to write the 4-th iterate:

$$v_4 = \tan 2\tan^{-1}\frac{\tan 2\tan^{-1}\frac{\tan 2\tan^{-1}\frac{\tan\frac{a^4\pi}{2}}{\tan\frac{a\pi}{2}}}{\tan 2\tan^{-1}\frac{\tan\frac{a^2\pi}{2}}{\tan\frac{a\pi}{2}}}}{\tan 2\tan^{-1}\frac{\tan 2\tan^{-1}\frac{\tan\frac{a^3\pi}{2}}{\tan\frac{a\pi}{2}}}{\tan 2\tan^{-1}\frac{\tan\frac{a^2\pi}{2}}{\tan\frac{a\pi}{2}}}}\ , \quad (6)$$

where we exploited the relationship $\vartheta_k(\omega) = 4\tan^{-1}\frac{\tan\frac{\omega}{2}}{v_k}$ for $-\pi < \omega < \pi$. For higher values of the index, the size of the "tangent tree" in (6) grows without bound. The analysis is not simplified by the fact that, by exploiting the identity

$$\tan 2\tan^{-1} x = \tfrac{2x}{1-x^2} \ ,$$

v_k may be put in rational form.

The simplicity of the limit in (5) is astonishing. Convergence of the parameter sequence to its limit is exponential. By Taylor expansion with respect to a it is possible to show that

$$v_k(a) = 2a + O(a^{2k-1}) \ .$$

A further consequence of Theorem 1 is that the map $\widetilde{\Omega}^{-1}(\omega)$ satisfies Schröder's equation $\widetilde{\Omega}^{-1}\circ\vartheta_\infty^{-1} = a\widetilde{\Omega}^{-1}$, where ϑ_∞^{-1} has parameter $v_\infty = 2a$. Any solution of this equation plays the fundamental role of eigenfunction of the composition operator with eigenvalue *a*. However, the solution of Schröder's equation is defined up to a constant factor. Since the product $\prod_{k=1}^{n}\frac{2a}{v_k}$ converges, the map

$$\Omega^{-1}(\omega) \equiv \lim_{n}\frac{\Omega_n^{-1}(\frac{\omega}{2})}{a^n} = \pi\frac{\widetilde{\Omega}^{-1}(\omega)}{\widetilde{\Omega}^{-1}(\pi)}$$

also satisfies Schröder's equation

$$\Omega^{-1}\circ\vartheta_\infty^{-1} = a\Omega^{-1} \ . \quad (7)$$

As we will show in the next section, Schröder's equation represents our starting point for defining continuous-time warped wavelets sharing the computational structure of our discrete-time warped wavelets, i.e., iterated warped filter banks based on the Laguerre transform.

The direct map $\Omega(\omega)$ satisfies the equation

$$\vartheta_\infty\circ\Omega(\omega) = \Omega(\tfrac{\omega}{a}) \ . \quad (8)$$

In other words, we have:

$$\vartheta_\infty^{-1}(\omega) = \Omega(a\Omega^{-1}(\omega)) \quad (9)$$

and

$$\vartheta_\infty(\omega) = \Omega(a^{-1}\Omega^{-1}(\omega)) \ . \quad (10)$$

These last two equations are conjugacy relationships; the composition of several ϑ_∞ or ϑ_∞^{-1} maps is conjugated, respectively, to negative or positive powers of the eigenvalue *a* via the eigenfunction and its inverse.

3. Scale-*a* Continuous-Time Wavelets

We showed in [6] that the construction of continuous-time warped wavelets is simplified if the sequence of warping parameters is constant. However, in this case, the required cutoff frequencies are attained only asymptotically. In this paper we provide an orthogonal and complete set of continuous-time warped wavelets exactly attaining exponential cutoff that are based on warping parameters constant over scale. Our construction is based on the results illustrated in the previous section.

We start by considering a scaling sequence $\phi_{N,m}(k)$ whose DFT is

$$\Phi_{N,m}(\omega) = e^{-j2m\Theta_N(\omega)}\prod_{k=1}^{N}\left\{\Lambda_{\infty,0}(2\Theta_{k-1}(\omega))H(\Theta_k(\omega))\right\}$$

where

$$\Theta_k(\omega) \equiv \tfrac{1}{2}\underbrace{\vartheta_\infty\circ\vartheta_\infty\circ\ldots\circ\vartheta_\infty}_{k-times}(\omega)$$

is the composition of asymptotic elementary maps. As is the case for any warped scaling functions in the form (1) with shift property (4), the set $\phi_{N,m}(k)$ is orthogonal for any positive integer *N* and for any choice of the warping parameters. Therefore,

$$\delta_{m,0} = \langle\phi_{N,m},\phi_{N,0}\rangle = \tfrac{1}{2\pi}\int_{-\pi}^{+\pi}\left|\Phi_{N,0}(\omega)\right|^2 e^{j2m\Theta_N(\omega)}d\omega \ .$$

By performing the change of variable $\omega = \Theta_N^{-1}(\frac{\alpha}{2})$ in the last integral and exploiting the fact that $-\Theta_N(-\pi) = \Theta_N(\pi) = 2^{N-1}\pi$, we obtain

$$\delta_{m,0} = \tfrac{1}{2\pi}\int_{-2^N\pi}^{+2^N\pi}\left|\Phi_{N,0}(\Theta_N^{-1}(\tfrac{\alpha}{2}))\right|^2 e^{jm\alpha}\frac{d\Theta_N^{-1}(\frac{\alpha}{2})}{d\alpha}d\alpha \ . \quad (11)$$

Since

$$\frac{d}{d\alpha}\vartheta_\infty^{-1}(\alpha) = \frac{1}{2\left|\Lambda_{\infty,0}(\vartheta_\infty^{-1}(\alpha))\right|^2} \ ,$$

then

$$\frac{d\Theta_N^{-1}(\frac{\alpha}{2})}{d\alpha} = \prod_{k=1}^{N}\frac{1}{2\left|\Lambda_{\infty,0}(\Theta_\infty^{-1}(\frac{\alpha}{2}))\right|^2} \ . \quad (12)$$

On the other hand, since $\Theta_k(\Theta_N^{-1}(\omega)) = \frac{1}{2}\Theta_{N-k}^{-1}(\omega)$ for $N \ge k$, with $\Theta_0^{-1}(\omega) \equiv 2\omega$, then

$$\Phi_{N,0}(\Theta_N^{-1}(\tfrac{\alpha}{2})) = \prod_{r=1}^{N}\left\{\Lambda_{\infty,0}(\Theta_r^{-1}(\tfrac{\alpha}{2}))H(\tfrac{1}{2}\Theta_{r-1}^{-1}(\tfrac{\alpha}{2}))\right\} \quad (13)$$

Substituting (12) and (13) in (11) we obtain:

$$\delta_{m,0} = \frac{1}{2\pi} \int_{-2^N\pi}^{+2^N\pi} e^{jm\alpha} \prod_{r=1}^{N} \frac{\left| H\left(\frac{1}{2}\Theta_{r-1}^{-1}\left(\frac{\alpha}{2}\right)\right)\right|^2}{2} \, d\alpha \;. \quad (14)$$

By repeated application of Schröder's equation one can show that

$$\Theta_{r-1}^{-1}\left(\tfrac{\omega}{2}\right) = \Omega\left(a^{r-1}\Omega^{-1}(\omega)\right).$$

Substituting this result in (14) we conclude that the continuous-time set $\tilde{\varphi}_{0,m}(t) = \tilde{\varphi}_{0,0}(t-m)$, where $\tilde{\varphi}_{0,0}(t)$ has FT:

$$\tilde{\Phi}_{0,0}(\omega) = \prod_{r=1}^{\infty} \frac{H\left(\frac{1}{2}\Omega\left(a^{r-1}\Omega^{-1}(\omega)\right)\right)}{\sqrt{2}} \quad (15)$$

is orthogonal:

$$\delta_{m,0} = \frac{1}{2\pi} \int_{-\infty}^{+\infty} e^{jm\omega} \left|\tilde{\Phi}_{0,0}(\omega)\right|^2 \, d\omega \;. \quad (16)$$

We remark that convergence of (14) as $N \to \infty$ can be established with a simple adaptation of the methods found in [12]. Notice that the arguments of H in the product (15) are in the form of conjugation to powers of the parameter a. Furthermore, $\tilde{\Phi}_{0,0}(\omega)$ satisfies the following warped two-scale equation:

$$\sqrt{2}\tilde{\Phi}_{0,0}(\vartheta_\infty(\omega)) = H\left(\tfrac{1}{2}\vartheta_\infty(\omega)\right)\tilde{\Phi}_{0,0}(\omega) \;. \quad (17)$$

By repeated use of this equation, one could define continuous-time warped wavelets based on the scaling function $\tilde{\varphi}_{0,0}(t)$, by letting

$$\tilde{\Phi}_{n,m}(\omega) = 2^{n/2}\tilde{\Phi}_{0,m}(2\Theta_n(\omega)) \,.$$

However, the half-bandwidth of the scaling function, essentially given by $\omega_n = \Theta_n^{-1}\left(\frac{\pi}{2}\right)$, according to the smallest bandwidth term in the defining product, does not meet the required power of a behavior as a function of scale.

In order to define continuous-time wavelets with exponential cutoff we consider scaling functions $\hat{\varphi}_{0,m}(t)$ having the following FT:

$$\hat{\Phi}_{0,m}(\omega) = \tilde{\Phi}_{0,m}(\Omega(\omega))\sqrt{\frac{d\Omega}{d\omega}}$$

Since Ω is increasing the derivative is positive and its square root real. Orthogonality of the set $\hat{\varphi}_{0,m}(t)$ may be checked by performing the variable change $\omega = \Omega(\alpha)$ in (16). Furthermore, $\hat{\varphi}_{0,m}(t)$ satisfies the following two-scale equation:

$$\frac{1}{\sqrt{a}}\hat{\Phi}_{0,0}\left(\tfrac{\omega}{a}\right) = \Lambda_{\infty,0}(\Omega(\omega))H\left(\tfrac{1}{2}\Omega\left(\tfrac{\omega}{a}\right)\right)\hat{\Phi}_{0,0}(\omega) \,. \quad (18)$$

By deriving both sides of identity (10) with respect to ω and changing ω into $\Omega(\omega)$ we obtain the following scaling rule for the derivative:

$$\Omega'\left(\tfrac{\omega}{a}\right) = a\,\vartheta'_\infty(\Omega(\omega))\,\Omega'(\omega) = 2a\left|\Lambda_{\infty,0}(\Omega(\omega))\right|^2\Omega'(\omega) \,.$$

The remaining part of (18) easily follows from (17).

Equation (18) is a remarkable result since it shows that the warped wavelets $\hat{\psi}_{n,m}(t)$ associated to the scaling function $\hat{\varphi}_{0,0}(t)$ are true scale-a wavelets. However, their "translates" are obtained by all-pass filtering rather than shifting. It is easy to check that the half-bandwidth of the scaling functions $\hat{\varphi}_{n,0}(t)$ attains exponential cutoff $a^n\pi$. In fact, the smallest bandwidth term is $H\left(\frac{1}{2}\Omega\left(\frac{\omega}{a^n}\right)\right)$ and since $\Omega(\pi) = \pi$ then $\frac{1}{2}\Omega\left(\frac{\omega_n}{a^n}\right) = \frac{\pi}{2}$ for $\omega_n = a^n\pi$.

Another important aspect of the set $\hat{\psi}_{n,m}(t)$ is that the structure needed to compute the expansion coefficients from the coefficients at scale 0 is identical to that needed for discrete warped wavelets, i.e., it is based on iterated warped filter banks, with constant parameters equal to $v_\infty = 2a$. This is so by virtue of the term $e^{-jm\Omega(\omega)}$ necessary for obtaining the "translates" of $\hat{\varphi}_{0,0}(t)$ in the frequency domain. Projection on the higher scale set requires only incremental Laguerre warping with phase characteristics $-\frac{\vartheta_\infty(\omega)}{2}$.

4. Self-Similarity

As shown in the previous section, in scale-a warped wavelets the map Ω, shown in Fig. 2, plays a fundamental role: it maps the points $a^{-n}\pi$ to the points $2^n\pi$. The map Ω has a complex functional form and this results in a fractal-like behavior. Quasi-self-similarity of the map Ω can be deduced from equation (8). If $\vartheta_\infty(\omega)$ is approximated to the first order by the linear map 2ω, we obtain:

$$2\Omega(\omega) \approx \Omega\left(\tfrac{\omega}{a}\right).$$

This approximation is more accurate for values of a close to 1/2.

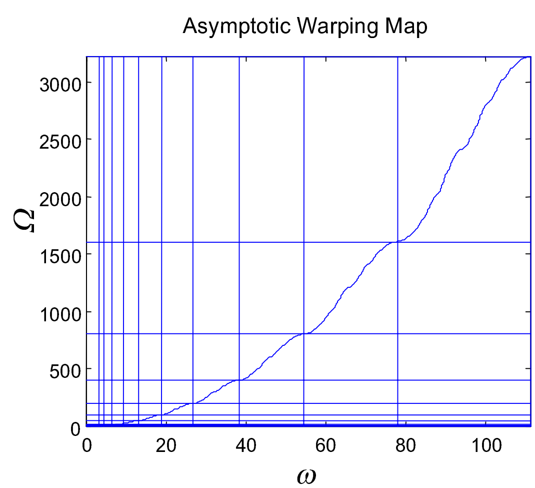

Fig. 2 *Asymptotic warping map showing quasi-self-similarity.*

It is interesting to note that with the iterated warping map one can build an exact self-similar function. Using Schröder's equation, it is possible to show that the sequence of functions $2^{-(n-1)}\Omega_n(\omega)$ converges, as $n \to \infty$, to a map $\Omega^\bullet(\omega)$ uniformly on any compact subset of $\Re$.

The map $\Omega^{\bullet}(\omega)$ is a-homogeneous in the sense given in [13], i.e., $\Omega^{\bullet}(a^m\omega) = a^{m\lambda}\Omega^{\bullet}(\omega) = 2^{-m}\Omega^{\bullet}(\omega)$, where $\lambda = -\log_a 2$. Note that

$$\Omega^{\bullet}(\omega) = \lim_n 2^{-(n-1)}\Omega_n(\omega),$$

while

$$\Omega(\omega) = \lim_n 2\Omega_n(a^n\omega).$$

Homogeneity of the map is a prerequisite for a real axis warping map directly converting dyadic wavelets to scale-a wavelets with a single map. In our construction the conversion map is updated at each scale and scale conversion is distributed. We must point out that the warping curve is determined only at the points $a^n\pi$, $n \in \mathbf{Z}$ in order to match the cutoff conditions. For example one could select the map

$$\omega \to \pi 2^{-\log_a(\frac{\omega}{\pi})}.$$

However, iterated Laguerre warping is the unique one-to-one warping that can be exactly implemented in rational filters.

5. Conclusions

In this paper we revisited the concept of frequency warped wavelets based on warped filter banks introduced in [6]. We sketched the theory of the construction based on Schröder's equation and Königs's model, which we generalized to parametric maps on the unit circle. We showed that the sequence of parameters for attaining exponential cutoff is rapidly converging to a simple limit. Furthermore, we showed that scale-a wavelets may be defined by means of warped wavelets. The structure required for computing the expansion coefficients is still given by iterated discrete warped filter banks and Laguerre warping is obtained by means of rational all-pass filters. Our scale-a warped wavelets are useful for arbitrarily improving the frequency resolution of the dyadic wavelets, crucial in many applications, such as speech and music processing. However, improved resolution is obtained at the cost of increased computational complexity, which is $O(N^2)$. Furthermore, the delay of the warped wavelet set is frequency dependent, obtaining curved diagrams in the time-frequency localization plane.

References

[1] P. W. Broome, "Discrete Orthonormal Sequences," *J. Assoc. Comput. Machinery,* vol. 12, no. 2, pp. 151-168, 1965.

[2] A. V. Oppenheim, D. H. Johnson and K. Steiglitz, "Computation of spectra with unequal resolution using the Fast Fourier Transform," *Proc. IEEE*, vol. 59, pp.299-301, Feb. 1971.

[3] R. G. Baraniuk and D. L. Jones, "Warped Wavelets Bases: Unitary Equivalence and Signal Processing," in *Proc. IEEE Int. Conf. Acoust., Speech, Signal Processing - ICASSP'93*, vol. III, pp. 320-323, 1993.

[4] T. Blu, "A New Design Algorithm for Two-Band Orthonormal Filter Banks and Orthonormal Rational Wavelets," *IEEE Trans. on Signal Processing*, vol. 46, no. 6, pp. 1494-1504, June 1998.

[5] G. Evangelista, "Pitch Synchronous Wavelet Representations of Speech and Music Signals," *IEEE Trans. on Signal Processing*, vol. 41, no.12, pp. 3313-3330, Dec. 1993.

[6] G. Evangelista and S. Cavaliere, "Discrete Frequency Warped Wavelets: Theory and Applications," *IEEE Transactions on Signal Processing*, special issue on Theory and Applications of Filter Banks and Wavelets, vol. 46, no. 4, pp.874-885, April 1998.

[7] G. Evangelista, S. Cavaliere, "Frequency Warped Filter Banks and Wavelet Transform: A Discrete-Time Approach Via Laguerre Expansions," *IEEE Transactions on Signal Processing*, vol. 46, no. 10, pp. 2638-2650, Oct. 1998.

[8] G. Evangelista, S.Cavaliere, "Auditory Modeling via Frequency Warped Wavelet Transform," *Proc. of the European Signal Processing Conference, EUSIPCO '98,* Rhodes, Greece, vol. I, pp. 117-120, Sept. 1998.

[9] S. Cavaliere, G. Evangelista, "Representation of Pseudoperiodic Signals by means of Pitch-Synchronous Frequency Warped Wavelet Transform," *Proc. of the European Signal Processing Conference, EUSIPCO '98, Rhodes, Greece, vol. II, pp. 625-628,* Sept. 1998.

[10] G. Evangelista, S. Cavaliere, "Arbitrary Bandwidth Wavelet Sets," *Proc. of IEEE Internat. Conference on Acoustics, Speech and Signal Processing, ICASSP '98*, Seattle, WA., vol. III, pp. 1801-1804, May 1998.

[11] J. H. Shapiro, "Composition Operators and Schröder's Functional Equation," Trans. of AMS, Contemporary Mathematics, no. 213, pp. 213-228, 1998.

[12] I. Daubechies, *Ten Lectures on Wavelets*, CBMS-NSF Reg. Conf. Series in Appl. Math., Phyladelphia, PA., SIAM, 1992.

[13] G. W. Wornell and A. V. Oppenheim, "Wavelet-Based Representations for a Class of Self-Similar Signals with Applications to Fractal Modulation," *IEEE Trans. Inform. Theory*, Vol. 38, No. 2, pp. 785-800, Mar. 1992.